atmosphere

Article

Identification and Characteristics of Historical Extreme High-Temperature Events over the China–Pakistan Economic Corridor

Tao Li [1,2,3] and Anming Bao [1,3,4,*]

1 State Key Laboratory of Desert and Oasis Ecology, Xinjiang Institute of Ecology and Geography, Chinese Academy of Sciences, Urumqi 830011, China
2 University of Chinese Academy of Sciences, Beijing 100049, China
3 Key Laboratory of GIS & RS Application Xinjiang Uygur Autonomous Region, Urumqi 830011, China
4 China-Pakistan Joint Research Center on Earth Sciences, CAS-HEC, Islamabad 45320, Pakistan
* Correspondence: baoam@ms.xjb.ac.cn

Abstract: Recently, there has been an increase in the occurrence of extreme high-temperature events across the China–Pakistan Economic Corridor (CPEC). Regional spatiotemporal identification and evaluation of extreme high temperatures are essential for accurate forecasting of future climate changes. When such events generate a meteorological hazard, it is important to understand their temporal and spatial features, return period, and identification criteria. Accurately identifying extreme events can help assess risk and predict their spatial–temporal variation. While past studies have focused on individual sites, extreme heat events generally manifest as spatially and temporally continuous regional events. In this study, we propose an objective identification technique based on gridded data and spatiotemporal continuity to reveal the spatiotemporal characteristics of intensity, frequency, and duration events of extreme heat events in the CPEC from May to October between 1961 and 2015. Furthermore, we estimate the return period of extreme heat in the study region using the generalized Pareto distribution (GPD). Our findings indicate that the historical extreme temperature events (intensity, frequency, and duration) in the CPEC have significantly increased. Areas with a high incidence of extreme heat events are concentrated in eastern Balochistan, northern Sindh, and southeastern Punjab. These findings suggest that disaster prevention and mitigation plans should be targeted towards areas with a high frequency of extreme heat events in the CPEC, allowing policy makers to better prepare for and respond to future events.

Keywords: extreme high-temperature event; spatial–temporal variation; generalized Pareto distribution; return period; China–Pakistan Economic Corridor

check for updates

Citation: Li, T.; Bao, A. Identification and Characteristics of Historical Extreme High-Temperature Events over the China–Pakistan Economic Corridor. *Atmosphere* **2023**, *14*, 530. https://doi.org/10.3390/atmos14030530

Academic Editors: Er Lu, Qingchen Chao and Hui Wang

Received: 8 February 2023
Revised: 5 March 2023
Accepted: 8 March 2023
Published: 9 March 2023

1. Introduction

Extreme weather and climate events, which include meteorological and hydrological disasters, have a significant impact on human society [1,2]. The IPCC Sixth Assessment Report indicates that global climate change will significantly increase the frequency, intensity, duration, and impact range of extreme weather and climate events, potentially increasing the rate at which they occur [3]. These events, which include extreme temperature events, droughts, rainstorms, floods, and other natural disasters, have caused substantial losses to the social economy and agricultural development, while also threatening human life and health [4–7]. For instance, in the summer of 2013, extreme temperature events in southeastern China broke a 141-year-old record and killed 1755 people in the Pudong area of Shanghai. In 2015, a high-temperature heat wave swept Pakistan's Karachi, killing over 1200 people, and hospitalizing around 65,000 individuals due to heatstroke [8,9]. According to the latest Lancet Countdown to China report, the death toll resulting from the heat wave quadrupled from 1990 to 26,800. causing an economic loss equivalent to the average annual income of 1.4 million Chinese [10]. Additionally, extreme heat events have significantly increased worldwide in recent decades [11]. Therefore, accurately identifying these extreme heat events and studying their changing characteristics, including recurrence periods, is crucial for assessing and managing the risk of such events.

Extreme climate events are typically regional phenomena with three-dimensional characteristics. They are characterized by a specific intensity, impact range, and duration [12,13]. However, most of the current studies on extreme heat events rely on single-station extreme thresholds or station thresholds within a fixed range for spatial and temporal characterization. The identification methods for extreme high-temperature events are mainly divided into three categories: the first is to define a single-station high-temperature threshold. When the temperature exceeds this threshold, it is defined as the occurrence of a single-station extreme high-temperature event [14]. The second method is to select a study area and define an extreme high-temperature event based on the regional average temperature sequence [15]. The third method is to first define a single-station extreme high temperature and then define an extreme event based on the range of the single-station extreme event [16]. However, the first and second types of methods are unable to define extreme high-temperature events that occur at different spatial scales. The third method is suitable for studying large-scale persistent extreme heat events. These methods for identifying extreme events rarely focus on the fact that extreme heat events are regional events with specific characteristics. In the study of drought, Dracup et al. [17] proposed that drought events are expressed by duration, intensity, and severity. Sheffield et al. [18] developed the previous research methods, and proposed the SAD (severity–area–duration) method to study global regional drought events from 1950 to 2000. However, this method is only applicable to drought events of fixed time duration and cannot achieve spatial migration. Ren et al. [19] proposed an objective identification method for persistent extreme events based on single sites or grid points. However, this method lacks the spatial extent and temporal continuity of events. Jing et al. [20] created the intensity–area–duration (IAD) method, which defines an extreme event as a collection of lattice points with a continuous area larger than a given threshold in a certain time scale. However, this method cannot fully characterize the dynamic process of a large-scale persistent extreme event and has the problem of repeatedly calculating the impact area of extreme events [21].

In the context of global climate change, the prediction of more severe heat wave events in various regions has significant impacts on human productive life [22,23]. Accurately predicting future extreme events is largely based on an assessment of long-term changes and trends in past extreme temperature events [24]. Therefore, understanding and analyzing long-term changes and trends in historical temperature extremes is essential for detecting and quantifying their adverse effects on human societies [25]. The CPEC, composed of China's Kashgar region and Pakistan, with more than 212 million inhabitants, is a pioneering demonstration area of the Belt and Road Initiative [26,27]. The region, with its diverse landscape and complex climate types, is prone to extreme weather and climate events that seriously threaten or even hinder the smooth implementation and operation of project construction. Moreover, the CPEC is one of the most densely populated regions globally, and extreme heat events can have severe ecological, demographic, social, and economic impacts on the area. Extreme heat events have attracted more attention among many extreme events since they significantly impact the social environment and people's lives. Several studies have shown that the CPEC region is highly sensitive to climate change due to global warming [28]. Previous studies have conducted a comprehensive analysis of extreme temperature changes in the CPEC based on site data [29]. However, a significant problem is that they mostly studied extreme temperature changes based on station data and extreme climate indices, with few studies on extreme events. Additionally, the limited data from traditional meteorological stations in the region cannot fully cover the entire area and cannot reflect the spatial differences in the distribution of high-temperature climates finely. They cannot also combine high-temperature heat waves with the spatial pattern of the landscape and population distribution. The predominantly arid climate and geographical location in the region of rapid temperature rise make the CPEC one of the most vulnerable regions globally to temperature rise, and those causing significant damage are generally extreme events. Therefore, studying the changes in extreme heat events in the CPEC based on grid point data is necessary. However, there are limitations in identifying extreme events, and hence, the purpose of this paper is to redefine and discriminate regional extreme heat events from a spatiotemporal continuum perspective by considering the spatiotemporal dynamics of extreme heat events. A method to identify extreme heat events based on grid point data is proposed, and a dataset of extreme low-temperature events in the CPEC has been produced, with the total number of dataset views and downloads exceeding 600 [30]. Moreover, no detailed study has been attempted so far to analyze extreme heat events in the CPEC. Therefore, this study has made progress in extending the target area, the extreme heat event study, and the heat recurrence period.

In order to better address the risks of extreme temperature events in the CPEC resulting from global warming, it is necessary to conduct a thorough analysis of the temporal and spatial changes, as well as the alteration of return periods, of extreme temperature events in the historical period. To address this knowledge gap, this study adopts the percentile method using daily maximum temperature data from the CPEC (1961–2015) to determine the threshold for extreme temperature events. Moreover, this study proposes a method for identifying extreme high-temperature events based on daily maximum temperature grid data. The study ultimately identifies the occurrence of extreme high-temperature events in the CPEC, discusses the temporal and spatial distribution characteristics of these events in the CPEC, and estimates the return period using the generalized Pareto distribution (GPD). This research answers three key questions: (1) How can an extreme high-temperature event be accurately identified? (2) What are the temporal and spatial changes in extreme high-temperature events in the CPEC? (3) What is the spatial distribution of the return period of extremely high-temperature events in the CPEC?

2. Materials and Methods

2.1. Study Area

The CPEC is situated in the northwest region of South Asia (SA), spanning between 23–41° N and 60–80° E. It stretches from Kashgar, China, to Gwadar Port, Pakistan, with a total length of 3000 km. The region comprises Balochistan, Sindh, Punjab, Khyber Pakhtunkhwa, Islamabad Capital District, Azad Kashmir (Pakistan-dominated Kashmir), Gilgit-Baltistan, and Kashgar, China (Figure 1). It is also linked to the “Silk Road Economic Belt” in the north and the “21st Century Maritime Silk Road” in the south, serving as a vital hub for connecting the North and South Silk Road and playing a significant role in the Belt and Road Initiative’s implementation [31,32]. The CPEC region is characterized by diverse climate types and complex geomorphic features. The northern high Himalayan region experiences an alpine mountainous climate, with frequent extreme low-temperature events and disasters. The mountainous and hilly areas of the temperate continental climate zone make up the central part. The vast Indus River plain covers the central region, mostly with a tropical monsoon climate, exhibiting high temperatures, heavy rainfall in summers, and frequent extreme high-temperature events and rainstorms. The geomorphic types of the region are complex and diverse [33,34]. The northern part of the region is mountainous and experiences an alpine mountainous climate, while the middle and southern parts are flat and open, with tropical grassland and a tropical desert climate, respectively. The study area has a hot and rainy summer and cold and dry in winter, with extreme low-temperature events mainly occurring in northern areas at high altitudes [30], and the extreme high-temperature events mainly occurring in the central and southeast areas [35].

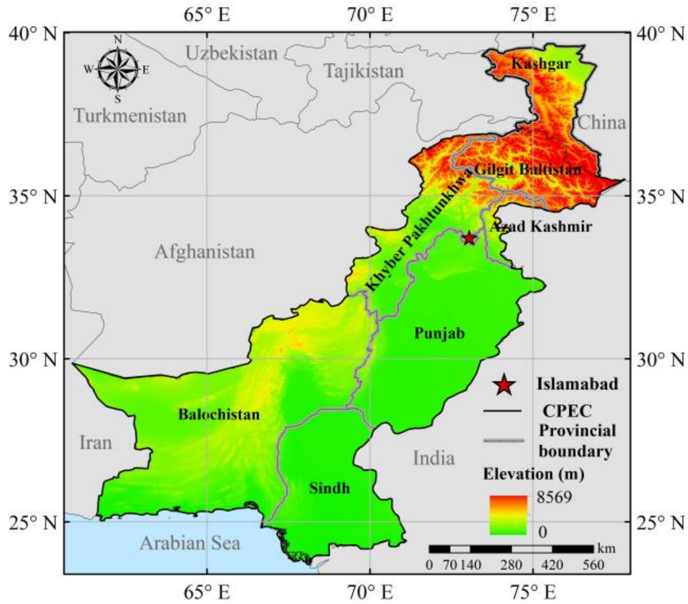

Figure 1. Sketch map of the China–Pakistan Economic Corridor (CPEC).

2.2. Data and Methods

2.2.1. Data

Historical maximum temperature data were used in this study. To calculate extreme high-temperature events, a daily meteorological dataset (maximum temperature) over the CPEC region for the period of 1961 to 2015 is used, which can be downloaded from the Science Data Bank [36]. The dataset was generated by interpolating weather station data with the ANUSPLIN software using latitude, longitude, and elevation as independent variables, which produced the lowest overall cross-validation. Three climate variables are included in the datasets on the Science Data Bank website: daily precipitation and maximum and minimum temperature. For this study, we utilized the daily maximum temperature data with a horizontal resolution of 0.25°.

2.2.2. Threshold Determination by Percentile Method

The definition of an extreme high-temperature threshold can be categorized into two types: relative and absolute thresholds [37]. Absolute thresholds, such as 30 °C, 35 °C, and 40 °C, are fixed values used to define extreme high-temperature events. Relative thresholds, on the other hand, are based on percentiles, such as the 90th, 95th, or 99th percentiles of the usual daily maximum temperature values in ascending order [38]. Considering the large topographic relief and regional temperature difference of the CPEC, the percentile threshold is used to define the threshold of extreme high-temperature events. In this study, after the cold mountain area with an average daily maximum temperature less than the average daily maximum temperature in the study area is excluded, the extreme high-temperature threshold is defined as the 95th percentile of the ascending order of the daily maximum temperature of the warm season (May–October) from 1961 to 2015, the spatial distribution of the extreme high-temperature threshold (Figure 2), and the blank area is the cold mountain area (the same below) [39–42]. In this study, a high-temperature event is defined as an extreme high-temperature event when the maximum daily temperature is exceeding the extreme high-temperature threshold and the average duration of many years is 3 or more days. The spatial distribution diagram of the extreme high-temperature threshold shows that the areas with the higher extreme high-temperature threshold of the CPEC are primarily concentrated in the north of Sindh, southwest of Punjab, and east and west of Balochistan, with the extreme high-temperature threshold exceeding 36 °C.

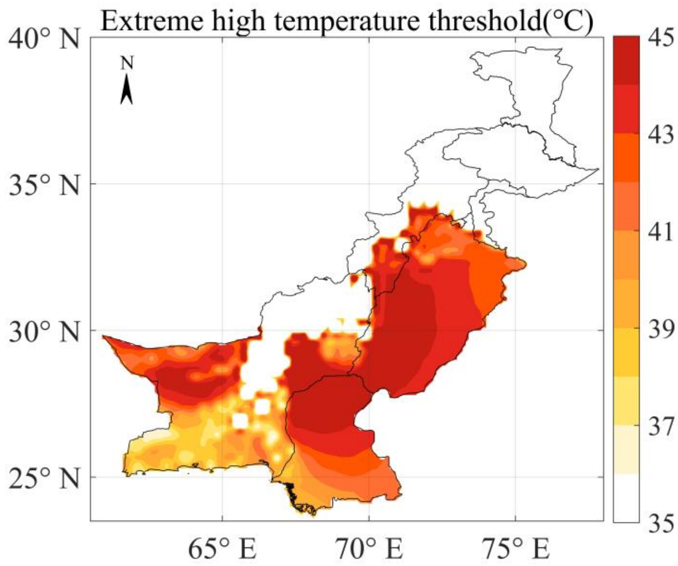

Figure 2. Spatial distribution of extreme high-temperature threshold in CPEC.

2.2.3. Identification of Extreme High-Temperature Events

Extreme high-temperature events exhibit three-dimensional characteristics in terms of their intensity, area of influence, and duration. Based on the intensity–area–duration (IAD) method, which defined an extreme event as a set of lattice points with a continuous area greater than a given threshold in a certain time scale [20,43,44]. However, this method has limitations in identifying extreme events with a fixed time scale and cannot account for the spatial migration of events, leading to repeated area calculations. Since an extreme high-temperature event changes continuously in both time and space, it is composed of multiple time states, each of which contains one or more extreme high-temperature objects. Thus, by following the extreme high-temperature objects with the topological intersection of adjacent time and space ranges, it is possible to extract and track extreme high-temperature events. By improving the original IAD three-dimensional recognition method, this paper proposes a method to identify extreme high-temperature events based on daily maximum temperature grid data and successfully identifies the extreme high-temperature event of the CPEC (Figure 3). The specific steps involved in the proposed method are as follows:

Step 1: Import the daily maximum temperature grid data. If the data are in point form, they should be converted to surface data (Latitude × Longitude × Time); if the imported data are surface data, proceed directly to Step 2.

Step 2: Calculate the extreme high-temperature threshold by excluding high and cold regions (areas where the average daily maximum temperature of the grid is lower than the average daily maximum temperature of the study area). The 95th percentile annual average of the daily maximum temperature series of the warm season (May to October) is used as the extreme high-temperature threshold. If the study area has no alpine region, proceed directly to Step 3. The calculation method of the extreme high-temperature threshold is variable, and can be defined according to research needs.

Step 3: Set the minimum impact area threshold A for extreme high-temperature events, and eliminate events with an impact area less than A. Although some errors may cause a small number of extreme high-temperature events, they will not result in disasters that affect the identification results. Therefore, the minimum area threshold A should be set. If the affected area of a high-temperature event is less than A, it shall be eliminated. This step first scans the entire time scale to eliminate extreme high-temperature events with temperatures less than A. In this paper, the minimum area A threshold is variable and can be set according to the size of the study area. For example, in the case of the CPEC, the minimum area A threshold is set to 25,000 km^2. It can be set to 150,000 km^2 for a Chinese-scale study and 500,000 for a global-scale study [18,45–47].

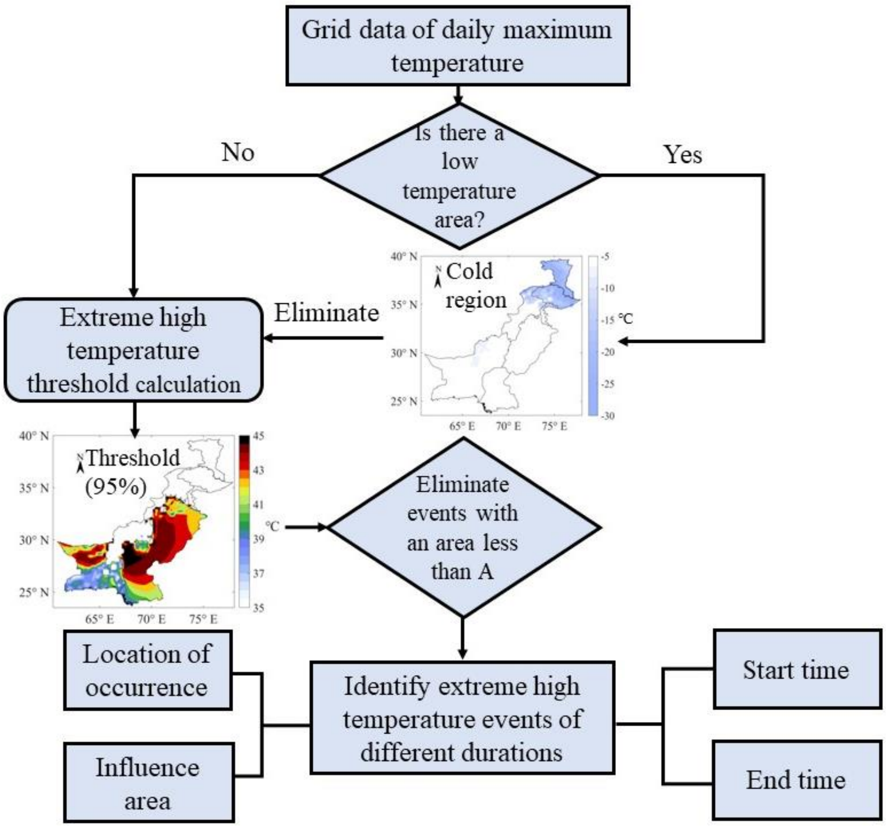

Figure 3. Extreme high-temperature events identification roadmap.

Step 4: Identify extreme high-temperature events. An extreme high-temperature event should include the processes of occurrence, development, and extinction. The development process includes the movement, splitting, and recombination of extreme high temperatures. Since the same extreme high-temperature event moves for a short period of time, there is spatial overlap during the development. Therefore, if the spatial extent topology of two extremely hot objects with adjacent time intersects, they are considered part of the same extremely hot event.

2.2.4. Definition of Intensity, Frequency, and Duration of Extreme High-Temperature Events

The spatial and temporal variation characteristics of extreme high-temperature events in the CPEC are quantified in three aspects: intensity, frequency, and duration (Table 1).

Table 1. Definition of intensity, frequency, and duration of extreme high-temperature events.

Essential Factor	Definition	Units
Strength	The intensity is the annual average maximum temperature of extreme high-temperature events	°C
Frequency	The frequency is the annual average number of extreme high-temperature events	times
Duration	The duration is the annual average duration of extreme high-temperature events	days

2.2.5. Generalized Pareto Distribution

The generalized Pareto distribution (GPD) is a POT stable distribution that filters the extremum based on a given threshold value and establishes the extremum distribution when a certain critical value is reached [48–52]. This distribution describes the characteristics of the probability distribution of all observed data over the threshold peak (POT).

The distribution function of GPD is:

$$\begin{cases} F(x) = 1 - \left[1 + \xi\left(\frac{x-\mu}{\sigma}\right)\right]^{-\frac{1}{\xi}}, x \geq \mu, \\ 1 + \xi((x-\mu)/\sigma) > 0 \end{cases} \tag{1}$$

where μ is a position parameter, $\sigma > 0$ is the scale parameter, and ξ is a shape parameter.

Return period refers to the average interval of meteorological and hydrological elements greater than or equal to a certain order of magnitude in the statistical period of recorded data in a certain year [53,54]. It is a wandering period in the sense of probability, which is essentially a small probability problem on the right side of the probability distribution.

Extreme value x under return period T for GPD distribution. The calculation formula of X_p is:

$$X_p = \mu - \frac{\sigma}{\xi}\left[1 - \left(\frac{1}{T}\right)^{-\xi}\right] \tag{2}$$

After the maximum likelihood estimation of parameters is obtained, the extreme value of the T-year return period can be obtained by substituting the estimated values of relevant parameters into the above formula X_p.

2.2.6. Significance Test

In this paper, the significance of the changing trend of the intensity, frequency, and duration of annual extreme high-temperature events is judged by a *t*-test.

3. Results

3.1. Identification Results of Extreme High-Temperature Events

This study proposes a method for identifying extreme high-temperature events using daily maximum temperature grid data. By applying this method, the extreme high-temperature events that occurred in the CPEC between 1961 and 2015 were identified. Figure 4 illustrates a 12-day extreme high-temperature event that took place in the CPEC. The event began on 1 October 2015, in the west of Balochistan, and reached its maximum impact on 8 October, covering the north of Balochistan. The highest temperature was recorded in the middle of Balochistan on 7 October, and ended on 12 October in Balochistan.

In this study, the typical persistent extreme high-temperature events that took place in the CPEC from 1961 to 2015 (Table 2). The table indicates that such long-lasting extreme high-temperature events predominantly occurred between May to July. By comparing the persistent high-temperature events over the years, it was found that the longest duration of a long-lasting extreme high-temperature event took place from 20 May 2014 to 2 July 2014, lasting for 44 days.

Table 2. Starting and ending time and duration of typical extreme high-temperature events in CPEC (1961−2015).

Serial Number	Extreme High-Temperature Events	
	Start and End Time	Duration (days)
1	1 May 1978–25 May 1978	25
2	2 June 1979–21 June 1979	20
3	27 May 1982–16 June1982	21

Table 2. *Cont.*

Serial Number	Extreme High-Temperature Events	
	Start and End Time	Duration (days)
4	16 May 1984–11 June 1984	27
5	8 May 1989–27 May 1989	21
6	5 June 1992–24 June 1992	20
7	25 May 1995–9 June 1995	16
8	29 May 2003–17 June 2003	20
9	11 May 2010–2 June 2010	23
10	12 May 2011–23 May 2011	11
12	19 July 2013–31 July 2013	13
13	20 May 2014–2 July 2014	44
14	20 June 2015–12 July 2015	30
15	1 October 2015–12 October 2015	12

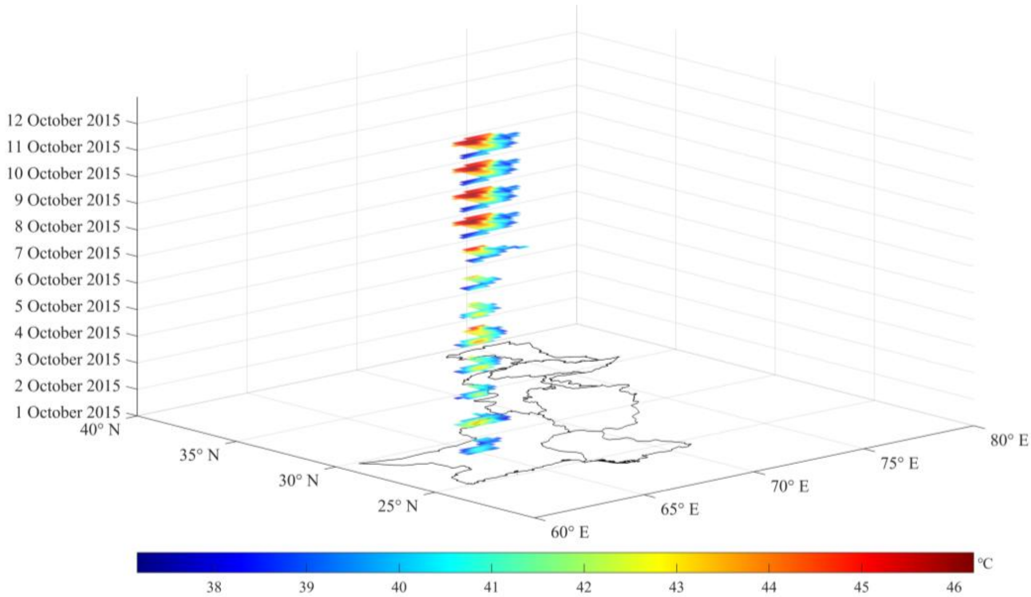

Figure 4. The extreme high-temperature event lasting for 12 days in the CPEC.

3.2. Time Variation of Extreme High-Temperature Events

Figure 5a displays the temporal variation trend of extreme high-temperature event intensity in the CPEC. The analysis indicates that the intensity of extreme high-temperature events in this region has shown an overall upward trend, with temperature increasing over time. Prior to 1971, temperatures decreased, but after that, they gradually increased. Figure 5b illustrates the frequency variation trend of extreme high-temperature events in the CPEC. The analysis shows that the frequency of extreme high-temperature events in this region generally shows an upward trend, and 1978 is a sudden change point. Before 1978, the growth rate was slow, while it was rapid after that year. Figure 5c presents the changing trend of the duration of extreme high-temperature events in the CPEC. The analysis shows that the duration of extreme high-temperature events in the region generally shows an upward trend. Before 1978, the duration was relatively short. The duration suddenly increased from 1978 to 1996, and the duration has generally increased since 1996. The highest multi-year average duration is about 7 days.

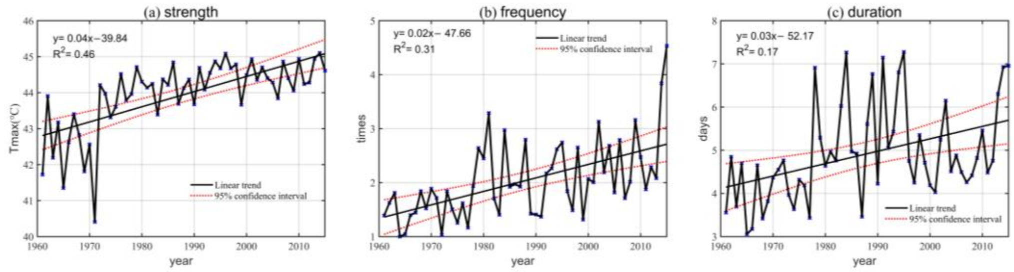

Figure 5. Time variation of extreme high-temperature events over the CPEC during 1961–2015: (**a**) strength; (**b**) frequency; (**c**) intensity (the straight line is a linear trend, and the red dotted line is a 95% confidence interval).

3.3. Spatial Variation of Extreme High-Temperature Events

Figure 6a illustrates the spatial variation of the multi-year average intensity of extreme high-temperature events in the CPEC. The analysis shows that the multi-year average intensity of extreme high-temperature events in this region is mainly distributed in the southern part of the CPEC, mainly including the whole province of Sindh, the western and eastern regions of Balochistan, and the central and southern regions of Punjab. The highest value of the multi-year average intensity is near Sindh and Balochistan. (Figure 6b) depicts the spatial distribution of the multi-year average frequency of extreme high-temperature events in the CPEC. The analysis shows that the multi-year average frequency of extreme high-temperature events in this region is mainly distributed in Sindh, Balochistan, and Punjab. The highest multi-year average frequency is in the west of Balochistan Province and the area near Karachi in the south of Sindh Province; Figure 6c displays the spatial change of the average multi-year duration of the extreme high-temperature events in the CPEC. The analysis shows that the average multi-year duration of the extreme high-temperature events in the region is mainly distributed in Sindh Province, Balochistan Province, and Punjab Province, and the region with the longest average multi-year duration is the southwest of Balochistan Province, the south of Punjab Province, and the area near Karachi in the south of Sindh Province.

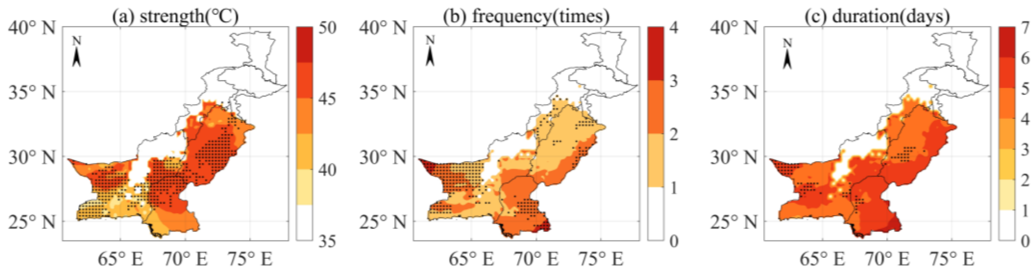

Figure 6. Time variation of extreme high-temperature events over the CPEC during 1961–2015: (**a**) strength; (**b**) frequency; (**c**) intensity. (Black dots represent where observer trends are significant ($p < 0.05$)).

3.4. Return Period Analysis

Figure 7 depicts the spatial distribution of the extreme high-temperature return levels for 5, 10, 50, and 100 years in the CPEC. It can be observed that the regions with high recurrence levels in these four recurrence periods are mainly concentrated in the areas around 30° N, and the extreme high temperature with a multi-year return period shows strong regionality. Overall, in the spatial distribution of 5, 10, 50, and 100 high-temperature return levels, the maximum return level of the CPEC is 50 °C

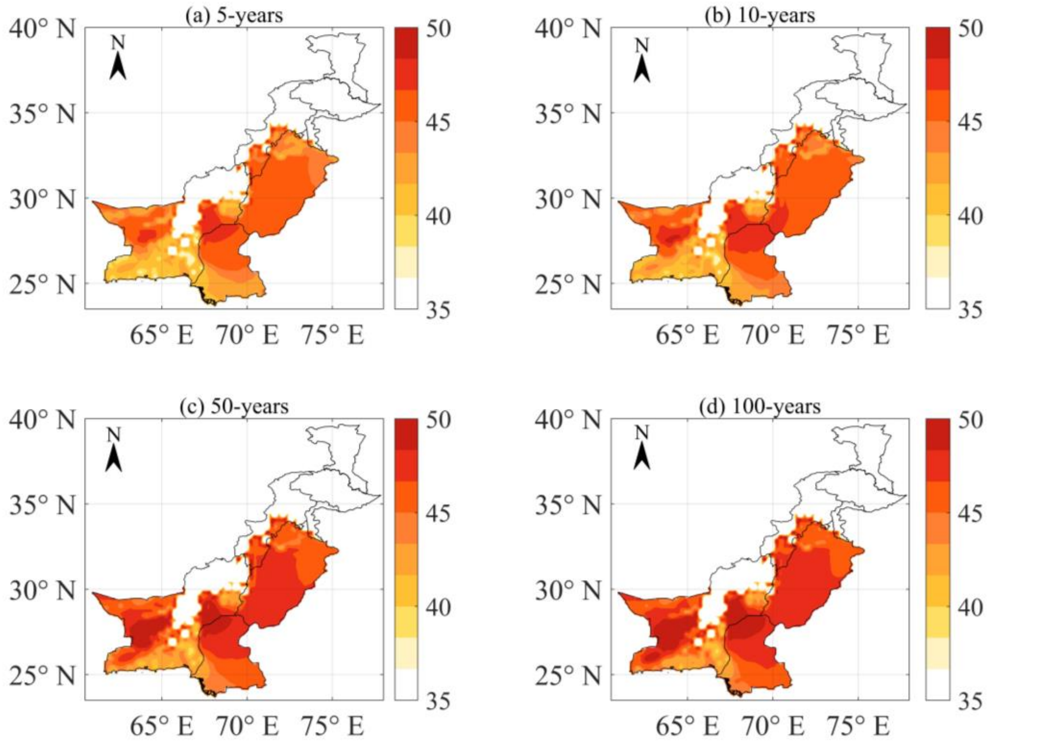

Figure 7. Spatial distribution of extreme high-temperature recurrence levels in CPEC: (**a**) 5a; (**b**) 10a; (**c**) 50a; (**d**) 100a.

4. Discussion

In the context of global warming, significant changes have occurred in the characteristics of atmospheric circulation, as well as the frequency and intensity of extreme high-temperature events, which have changed significantly. Thus, it is essential to strengthen research and analysis in this field to improve our understanding of the level of extreme high-temperature events. Furthermore, as the ecosystem gradually adapts to the warm climate in the future, vulnerability to extreme high-temperature events will also gradually increase [55–58]. When high-intensity, extreme high-temperature events occur, they will have significant and long-term impacts on the structure and function of the ecosystem [59]. However, one limitation of this study is that the temporal variation of extreme high-temperature events indicates abrupt change points in 1970 (Figure 5a–c), and the underlying reasons for this phenomenon need further investigation. Therefore, it is necessary to study the characteristics of spatial and temporal variation and return period analysis of extreme high temperatures from the perspective of disaster-causing factors for assessing regional meteorological and hydrological disasters. Furthermore, it is crucial to investigate the causes of sudden changes in time and space in the region and analyze the risk of the CPEC region in combination with disaster-causing factors such as population, economy, and cultivated land [60–62]. This may help develop a more comprehensive analysis to inform the prevention and control of natural disasters in the CPEC.

Due to the escalating frequency of extreme weather events, various domains, including socioeconomic, environmental, ecosystem, and human health, have been adversely impacted [63–65]. Hence, the causes of extreme climate events are increasingly becoming a critical area of study for numerous scholars. In previous research on extreme heat events in the CPEC, scholars relied on site data and the extreme climate index proposed by ETCCDI. However, due to the limited availability of site information in the CPEC, the accuracy of the findings may have been impacted. Ullah et al. (2019) conducted a study on the diurnal heat waves in Pakistan, revealing that the southern, central, and eastern regions experience high heat waves [66]. Monteiro and Caballero. (2019) studied extreme wet bulb temperature events in southern Pakistan and found that these events were connected to an abnormal inflow of marine air from the Arabian Sea into the Indus basin, and that land-use changes also had a significant impact on modifying the conditions for such extreme events [67]. In a recent study, Saleem et al. (2021) delved into the causes of extreme temperatures in Pakistan and found that the intensity of La Niña in the western Pacific Ocean and the Southern Oscillation are strongly linked to the intensity of extreme heat events in the region [68].

The escalation in extreme heat events in the CPEC may stem from a range of factors, including topographic conditions, rapid urbanization, deforestation, population expansion, and other anthropogenic factors [69]. Pakistan, being the world's fifth most populous nation, is experiencing a steady population rise. Regions with high population densities in Pakistan, such as Sindh, western Balochistan, and southeastern Punjab, are also the areas identified in this study as having high rates of extreme heat events in the CPEC. These regions will face more frequent and severe heat waves in the future, potentially causing significant damage to the country's economy [70–72]. Based on the study's results, it is recommended that high-temperature disaster preparedness and mitigation policies be tailored specifically towards the areas of Sindh, western Balochistan, and southeastern Punjab. This targeted approach will reduce the country's exposure to high-temperature heat waves [73].

Based on the spatial distribution map of extreme high-temperature events and the spatial distribution of return periods in this study, the border regions of Sindh, Balochistan, and Punjab provinces are projected to become the next hotspot for frequent extreme heat events. Therefore, it is crucial for the local government to closely monitor early warning systems for extreme high-temperature events in the region, mitigating risks associated with these events [34]. The CPEC, being a crucial area for infrastructure projects such as oil and gas pipelines and road transportation, is especially vulnerable to extreme high temperatures, making it more susceptible to risks in the future.

From a perspective of spatial and temporal continuity of extreme heat events, this study employs a novel research framework to identify regional extreme heat events that accurately and reliably determine the start time, end time, and occurrence range of extreme heat events and other characteristics. However, the study also acknowledges that there are certain limitations. The identification method of regional extreme heat events is dependent on the definition of extreme heat thresholds and the determination of minimum area thresholds. As a result, the choice of these parameters will unavoidably impact the identification of some regional extreme heat events since these parameters are variable. Nevertheless, the extreme heat events identified in this paper for the CPEC confirm the accuracy of the proposed method for identifying extreme heat events. This confirmation was achieved through a comparison with various sources in the region, including news reports, Pakistan Weather Portal (PWP), research papers [68,74,75], newspapers and magazines, and the international disaster database (EM-DAT). Therefore, researchers can conduct regional extreme heat event studies based on their research requirements.

5. Conclusions

Extreme thermal events refer to the occurrence of extreme phenomena not only at individual points but also to a certain range and duration of impact. The ETCCDI has defined 27 extreme climate indices, which are widely used, but they only apply to extreme phenomena at other points (stations or grid points). It is commonly understood that extreme heat events are regional phenomena with a certain range of influence and duration. Therefore, this study utilizes grid point data and a newly proposed technique for objectively identifying extreme heat events based on spatial and temporal dynamics. The study analyzes the daily maximum temperatures of the China–Pakistan Economic Corridor for the last 55 years and discusses their spatial and temporal variability characteristics and the spatial distribution of recurrence periods of extreme high temperatures.

From 1961 to 2015, there were discernible differences in the spatial distribution of the threshold, intensity, frequency, and duration of extreme high-temperature events in the

CPEC. The locations with the highest benchmark value of extreme high-temperature events were predominantly situated in the north of Sindh Province, south of Punjab Province, and east of Balochistan Province. In terms of temporal changes, there was a clear increase in the intensity, frequency, and duration of extreme high-temperature events in this region This finding is consistent with the global climate warming trend. Furthermore, in terms of spatial change, the locations with the highest intensity of extreme high-temperature events were mostly concentrated between the northern parts of Sindh Province and the Balochistan Province, where the temperature can reach up to 50 °C. Additionally, the places with the highest frequency of extreme high-temperature events were located in the far west of Balochistan Province and the far south of Sindh Province. The duration of extreme high-temperature events was roughly equivalent to the frequency of high-temperature events, but the former had a broader spatial scope. The highest values for the duration of extreme high-temperature events also consistently occurred in the western part of Balochistan, the southern part of Sindh, and the southeastern part of Punjab.

The assessment of the return period of extreme temperature in the CPEC suggests that the generalized Pareto distribution can be used to fit the daily maximum temperature data. The spatial distribution of the return level of extreme temperature across return periods indicates that extreme temperatures are highly localized. Additionally, with an increase in the number of return periods, the territorial extent of the area with high return levels gradually expands. Based on the spatial distribution diagram of the return level of extreme high temperature, the intersection of Sindh and Balochistan experiences an abrupt shift in the 10a return period, where a region with high return levels emerges, and its spatial extent continues to grow during the 50a and 100a return periods.

Although previous studies have documented an increase in the intensity, frequency, and duration of extreme heat events in the China–Pakistan Economic Corridor (CPEC), most have analyzed their variability using ETCCDI indices or station data. Few studies have investigated extreme heat events from the perspective of regional events. In this study, we adopt a novel research approach to identify regional extreme heat events based on their spatial and temporal continuity. Our findings show that historical extreme heat events ($\geq$20 d) in the CPEC occurred mainly in 1978, 1979, 1982, 1984, 1989, 1992, 2003, 2010, 2014, and 2015. Among them, the extreme heat event that occurred from late June to early July 2015 is considered one of the most extreme heat events on record in the region and one of the deadliest [76,77]. Our study identified this event with complete accuracy using a 30-day duration from 3 June to 12 July 2015, and it is listed in Table 2 under the identification event method of this study.

Author Contributions: All authors were involved in the intellectual elements of this paper. T.L. conceived the idea of the study and designed the research, wrote the paper, discussed the results, and revised the manuscript; A.B. conceived the idea of the study and designed the research, discussed the results, and revised the manuscript. All authors have read and agreed to the published version of the manuscript.

Funding: This study was jointly supported by the Strategic Priority Research Program of the Chinese Academy of Sciences (Grant No. XDA20030101), Transformation of Scientific and Technological Achievements from the Qinghai Province (Grant No. 2020-SF-145), The 2020 Qinghai Kunlun talents-Leading scientists project (Grant No. 2020-LCJ-02), Key program of International Cooperation, Bureau of International Cooperation, Chinese Academy of Sciences (Grant No. 131551KYSB20210030).

Institutional Review Board Statement: Not applicable.

Informed Consent Statement: Not applicable.

Data Availability Statement: The data presented in this study are available on request from the corresponding author.

Conflicts of Interest: The authors declare no conflict of interest.

References

1. Lesk, C.; Rowhani, P.; Ramankutty, N. Influence of extreme weather disasters on global crop production. *Nature* **2016**, *529*, 84–87. [CrossRef] [PubMed]
2. Jain, P.; Castellanos-Acuna, D.; Coogan, S.C.P.; Abatzoglou, J.T.; Flannigan, M.D. Observed increases in extreme fire weather driven by atmospheric humidity and temperature. *Nat. Clim. Chang.* **2022**, *12*, 63–70. [CrossRef]
3. Arias, P.; Bellouin, N.; Coppola, E.; Jones, R.; Krinner, G.; Marotzke, J.; Naik, V.; Palmer, M.; Plattner, G.K.; Rogelj, J.; et al. Climate Change 2021: The Physical Science Basis. Contribution of Working Group I to the Sixth Assessment Report of the Intergovernmental Panel on Climate Change. In Proceedings of the 2021 Intergovernmental Panel on Climate Change AR6, Remote, 26 July–7 August 2021.
4. Oudin Åström, D.; Forsberg, B.; Ebi, K.L.; Rocklöv, J. Attributing mortality from extreme temperatures to climate change in stockholm, sweden. *Nat. Clim. Chang.* **2013**, *3*, 1050–1054. [CrossRef]
5. Dunne, J.P.; Stouffer, R.J.; John, J.G. Reductions in labour capacity from heat stress under climate warming. *Nat. Clim. Chang.* **2013**, *3*, 563–566. [CrossRef]
6. Wernberg, T.; Smale, D.A.; Tuya, F.; Thomsen, M.S.; Langlois, T.J.; de Bettignies, T.; Bennett, S.; Rousseaux, C.S. An extreme climatic event alters marine ecosystem structure in a global biodiversity hotspot. *Nat. Clim. Chang.* **2013**, *3*, 78–82. [CrossRef]
7. Palmer, T. Record-breaking winters and global climate change. *Science* **2014**, *344*, 803–804. [CrossRef]
8. Hussain, M.; Butt, A.R.; Uzma, F.; Ahmed, R.; Irshad, S.; Rehman, A.; Yousaf, B. A comprehensive review of climate change impacts, adaptation, and mitigation on environmental and natural calamities in pakistan. *Environ. Monit. Assess.* **2020**, *192*, 48. [CrossRef]
9. Sun, X.; Sun, Q.; Zhou, X.; Li, X.; Yang, M.; Yu, A.; Geng, F. Heat wave impact on mortality in pudong new area, china in 2013. *Sci. Total Environ.* **2014**, *493*, 789–794. [CrossRef]
10. Cai, W.; Zhang, C.; Suen, H.P.; Ai, S.; Bai, Y.; Bao, J.; Chen, B.; Cheng, L.; Cui, X.; Dai, H.; et al. The 2020 china report of the lancet countdown on health and climate change. *Lancet Public Health* **2021**, *6*, e64–e81. [CrossRef]
11. Wang, C.; Zheng, J.; Lin, W.; Wang, Y. Unprecedented heatwave in western north america during late june of 2021: Roles of atmospheric circulation and global warming. *Adv. Atmos. Sci.* **2022**, *40*, 14–28. [CrossRef]
12. Lyon, B.; Barnston, A.G.; Coffel, E.; Horton, R.M. Projected increase in the spatial extent of contiguous us summer heat waves and associated attributes. *Environ. Res. Lett.* **2019**, *14*, 114029. [CrossRef]
13. Keellings, D.; Moradkhani, H. Spatiotemporal evolution of heat wave severity and coverage across the united states. *Geophys. Res. Lett.* **2020**, *47*. [CrossRef]
14. Yan, Z.; Jones, P.D.; Davies, T.D.; Moberg, A.; Bergström, H.; Camuffo, D.; Cocheo, C.; Maugeri, M.; Demarée, G.R.; Verhoeve, T.; et al. Trends of extreme temperatures in europe and china based on daily observations. *Clim. Chang.* **2002**, *1*, 355–392. [CrossRef]
15. Walsh, J.E.; Phillips, A.S.; Portis, D.H.; Chapman, W.L. Extreme cold outbreaks in the United States and Europe, 1948–1999. *J. Clim.* **2001**, *14*, 2642–2658. [CrossRef]
16. Wang, Y.; Ren, F.; Zhang, X. Spatial and temporal variations of regional high temperature events in china. *Int. J. Climatol.* **2014**, *34*, 3054–3065. [CrossRef]
17. John, A.; Dracup; Seong, L.K.; Edwin, G.; Paulson, J. On the definition of droughts. *Water Resour. Res.* **1980**, *16*, 297–302.
18. Sheffield, J.; Andreadis, K.M.; Wood, E.F.; Lettenmaier, D.P. Global and continental drought in the second half of the twentieth century: Severity–area–duration analysis and temporal variability of large-scale events. *J. Clim.* **2009**, *22*, 1962–1981. [CrossRef]
19. Ren, F.; Cui, D.; Gong, Z.; Wang, Y.; Zou, X.; Li, Y.; Wang, S.; Wang, X. An objective identification technique for regional extreme events. *J. Clim.* **2012**, *25*, 7015–7027. [CrossRef]
20. Cheng, J.; Tong, J.; Yanjun, W.; Jing, C.; Dongnan, J.; Lanxin, L.; Buda, S.U. A study on regional extreme precipitation events and the exposure of population and economy in china. *Acta Meteorol. Sin.* **2016**, *74*, 572–582.
21. Wang, A.; Wang, Y.; Su, B.; Kundzewicz, Z.W.; Tao, H.; Wen, S.; Qin, J.; Gong, Y.; Jiang, T. Comparison of changing population exposure to droughts in river basins of the tarim and the indus. *Earth's Future* **2020**, *8*, e2019EF001448. [CrossRef]
22. Fischer, E.M.; Sippel, S.; Knutti, R. Increasing probability of record-shattering climate extremes. *Nat. Clim. Chang.* **2021**, *11*, 689–695. [CrossRef]
23. Arnold, C. Death by climate change. *Nat. Clim. Chang.* **2022**, *12*, 607–609. [CrossRef]
24. Grotjahn, R.; Black, R.; Leung, R.; Wehner, M.F.; Barlow, M.; Bosilovich, M.; Gershunov, A.; Gutowski, W.J.; Gyakum, J.R.; Katz, R.W.; et al. North American extreme temperature events and related large scale meteorological patterns: A review of statistical methods, dynamics, modeling, and trends. *Clim. Dyn.* **2016**, *46*, 1151–1184. [CrossRef]
25. Sun, X.; Ren, G.; Shrestha, A.B.; Ren, Y.; You, Q.; Zhan, Y.; Xu, Y.; Rajbhandari, R. Changes in extreme temperature events over the Hindu Kush Himalaya during 1961–2015. *Adv. Clim. Chang. Res.* **2017**, *8*, 157–165. [CrossRef]
26. Ali, S.; Eum, H.; Cho, J.; Dan, L.; Khan, F.; Dairaku, K.; Shrestha, M.L.; Hwang, S.; Nasim, W.; Khan, I.A.; et al. Assessment of climate extremes in future projections downscaled by multiple statistical downscaling methods over Pakistan. *Atmos. Res.* **2019**, *222*, 114–133. [CrossRef]
27. Zeng, D.; Wu, J.; Mu, Y.; Li, H.; Deng, M.; Wei, Y.; Sun, W. An assessment of tourism climate comfort in the China–Pakistan economic corridor. *Sustainability* **2020**, *12*, 6981. [CrossRef]
28. Abid, M.; Schilling, J.; Scheffran, J.; Zulfiqar, F. Climate change vulnerability, adaptation and risk perceptions at farm level in Punjab, Pakistan. *Sci. Total Environ.* **2016**, *547*, 447–460. [CrossRef]

29. Ullah, S.; You, Q.; Ullah, W.; Ali, A.; Xie, W.; Xie, X. Observed changes in temperature extremes over China-Pakistan economic corridor during 1980–2016. *Int. J. Climatol.* **2019**, *39*, 1457–1475. [CrossRef]
30. Li, T.; Tao, H.; Chen, J. A gridded dataset of extremely low-temperature events in the China-Pakistan economic corridor during 1961–2015. *China Sci. Data* **2021**, *6*, 33–42. [CrossRef]
31. Khan, M.; Mahmood, A.; Shoaib, M. Role of ethical leadership in improving employee outcomes through the work environment, work-life quality and ICT skills: A setting of China-Pakistan economic corridor. *Sustainability* **2022**, *14*, 11055. [CrossRef]
32. Shelton, S.; Dixon, R.D. Long-term seasonal drought trends in the China-Pakistan economic corridor. *Climate* **2023**, *11*, 45. [CrossRef]
33. Iqbal, M.F.; Athar, H. Validation of satellite based precipitation over diverse topography of Pakistan. *Atmos. Res.* **2018**, *201*, 247–260. [CrossRef]
34. Khan, N.; Shahid, S.; Ismail, T.B.; Wang, X. Spatial distribution of unidirectional trends in temperature and temperature extremes in Pakistan. *Theor. Appl. Climatol.* **2019**, *136*, 899–913. [CrossRef]
35. Khan, N.; Shahid, S.; Ahmed, K.; Wang, X.; Ali, R.; Ismail, T.; Nawaz, N. Selection of GCMs for the projection of spatial distribution of heat waves in Pakistan. *Atmos. Res.* **2020**, *233*, 104688. [CrossRef]
36. Chen, J.; Tao, H.; Liu, J. A daily meteorological dataset in China-Pakistan economic corridor from 1961 to 2015. *Sci. Data Bank* **2021**, *6*, 229–238.
37. Zhai, P.; Pan, X. Change in extreme temperature and precipitation over northern China during the second half of the 20th century. *Acta Geogr. Sin.* **2003**, *58*, 1–10.
38. Fan, L.; Yan, Z.; Chen, D.; Li, Z. Assessment of central asian heat extremes by statistical downscaling: Validation and future projection for 2015–2100. *Adv. Clim. Chang. Res.* **2022**, *13*, 14–27. [CrossRef]
39. Lv, Y.; Jiang, T.; Tao, H.; Zhai, J.; Wang, Y. Spatial-temporal patterns of population exposed to the extreme maximum temperature events in the belt and road regions. *Sci. Technol. Rev.* **2020**, *38*, 68–79.
40. Zheng, B.; Chenu, K.; Fernanda Dreccer, M.; Chapman, S.C. Breeding for the future: What are the potential impacts of future frost and heat events on sowing and flowering time requirements for Australian bread wheat (*Triticum aestivium*) varieties? *Glob. Change Biol.* **2012**, *18*, 2899–2914. [CrossRef]
41. Coma, R.; Ribes, M.; Serrano, E.; Jiménez, E.; Salat, J.; Pascual, J. Global warming-enhanced stratification and mass mortality events in the Mediterranean. *Proc. Natl. Acad. Sci. USA* **2009**, *106*, 6176–6181. [CrossRef]
42. Mazdiyasni, O.; Aghakouchak, A. Substantial increase in concurrent droughts and heatwaves in the United States. *Proc. Natl. Acad. Sci. USA* **2015**, *112*, 11484–11489. [CrossRef] [PubMed]
43. Zhai, J.; Huang, J.; Su, B.; Cao, L.; Wang, Y.; Jiang, T.; Fischer, T. Intensity–area–duration analysis of droughts in China 1960–2013. *Clim. Dyn.* **2017**, *48*, 151–168. [CrossRef]
44. Wen, S.; Wang, A.; Tao, H.; Malik, K.; Huang, J.; Zhai, J.; Jing, C.; Rasul, G.; Su, B. Population exposed to drought under the 1.5 °C and 2.0 °C warming in the Indus river basin. *Atmos. Res.* **2019**, *218*, 296–305. [CrossRef]
45. Wang, A.; Lettenmaier, D.P.; Sheffield, J. Soil moisture drought in China, 1950–2006. *J. Clim.* **2011**, *24*, 3257–3271. [CrossRef]
46. Lloyd-Hughes, B. A spatio-temporal structure-based approach to drought characterisation. *Int. J. Climatol.* **2012**, *32*, 406–418. [CrossRef]
47. Xu, K.; Yang, D.; Yang, H.; Li, Z.; Qin, Y.; Shen, Y. Spatio-temporal variation of drought in China during 1961–2012: A climatic perspective. *J. Hydrol.* **2015**, *526*, 253–264. [CrossRef]
48. El Rafei, M.; Sherwood, S.; Evans, J.P.; Ji, F. Analysis of extreme wind gusts using a high-resolution Australian regional reanalysis. *Weather Clim. Extrem.* **2023**, *39*, 100537. [CrossRef]
49. Rivoire, P.; Le Gall, P.; Favre, A.; Naveau, P.; Olivia Martius, A.D. High return level estimates of daily era-5 precipitation in Europe estimated using regionalized extreme value distributions. *Weather Clim. Extrem.* **2022**, *38*, 100500. [CrossRef]
50. Singirankabo, E.; Iyamuremye, E. Modelling extreme rainfall events in kigali city using generalized pareto distribution. *Meteorol. Appl.* **2022**, *29*, e2076. [CrossRef]
51. Rodrigues, D.T.; Gonçalves, W.A.; Spyrides, M.H.C.; Santos E Silva, C.M.; Souza, D.O. Spatial distribution of the level of return of extreme precipitation events in northeast Brazil. *Int. J. Climatol.* **2020**, *40*, 5098–5113. [CrossRef]
52. Tebaldi, C.; Strauss, B.H.; Zervas, C.E. Modelling sea level rise impacts on storm surges along us coasts. *Environ. Res. Lett.* **2012**, *7*, 14011–14032. [CrossRef]
53. Mizuta, R.; Endo, H. Projected changes in extreme precipitation in a 60-km agcm large ensemble and their dependence on return periods. *Geophys. Res. Lett.* **2020**, *47*, e2019GL086855. [CrossRef]
54. Raschke, M. About the return period of a catastrophe. *Nat. Hazards Earth Syst. Sci.* **2022**, *22*, 245–263. [CrossRef]
55. Bastos, A.; Ciais, P.; Friedlingstein, P.; Sitch, S.; Pongratz, J.; Fan, L.; Wigneron, J.P.; Weber, U.; Reichstein, M.; Fu, Z.; et al. Direct and seasonal legacy effects of the 2018 heat wave and drought on european ecosystem productivity. *Sci. Adv.* **2020**, *6*, a2714–a2724. [CrossRef]
56. El-Madany, T.S.; Carrara, A.; Martín, M.P.; Moreno, G.; Kolle, O.; Pacheco-Labrador, J.; Weber, U.; Wutzler, T.; Migliavacca, M.R. Mirco Drought and heatwave impacts on semi-arid ecosystems' carbon fluxes along a precipitation gradient. *Philos. Trans. R. Soc. B Biol. Sci.* **2020**, *375*, 20190519. [CrossRef]
57. Zampieri, M.; Russo, S.; di Sabatino, S.; Michetti, M.; Scoccimarro, E.; Gualdi, S. Global assessment of heat wave magnitudes from 1901 to 2010 and implications for the river discharge of the alps. *Sci. Total Environ.* **2016**, *571*, 1330–1339. [CrossRef]

58. Yang, Z.; Yang, B.; Liu, P.; Zhang, Y.; Hou, L.; Yuan, X. Exposure to extreme climate decreases self-rated health score: Large-scale survey evidence from china. *Glob. Environ. Chang.* **2022**, *74*, 102514. [CrossRef]
59. Piao, S.; Zhang, X.; Chen, A.; Liu, Q.; Lian, X.; Wang, X.; Peng, S.; Wu, X. The impacts of climate extremes on the terrestrial carbon cycle: A review. *Sci. China Earth Sci.* **2019**, *62*, 1551–1563. [CrossRef]
60. Chambers, J. Global and cross-country analysis of exposure of vulnerable populations to heatwaves from 1980 to 2018. *Clim. Chang.* **2020**, *163*, 539–558. [CrossRef]
61. Jones, B.; O Neill, B.C.; Mcdaniel, L.; Mcginnis, S.; Mearns, L.O.; Tebaldi, C. Future population exposure to us heat extremes. *Nat. Clim. Chang.* **2015**, *5*, 652–655. [CrossRef]
62. Tuholske, C.; Caylor, K.; Funk, C.; Verdin, A.; Sweeney, S.; Grace, K.; Peterson, P.; Evans, T. Global urban population exposure to extreme heat. *Proc. Natl. Acad. Sci. USA* **2021**, *118*, e2024792118. [CrossRef] [PubMed]
63. Bellprat, O.; Guemas, V.; Doblas-Reyes, F.; Donat, M.G. Towards reliable extreme weather and climate event attribution. *Nat. Commun.* **2019**, *10*, 1732. [CrossRef] [PubMed]
64. Faranda, D.; Vrac, M.; Yiou, P.; Jézéquel, A.; Thao, S. Changes in future synoptic circulation patterns: Consequences for extreme event attribution. *Geophys. Res. Lett.* **2020**, *47*, e2020GL088002. [CrossRef]
65. Perkins-Kirkpatrick, S.E.; Stone, D.A.; Mitchell, D.M.; Rosier, S.; King, A.D.; Lo, Y.T.E.; Pastor-Paz, J.; Frame, D.; Wehner, M. On the attribution of the impacts of extreme weather events to anthropogenic climate change. *Environ. Res. Lett.* **2022**, *17*, 24009. [CrossRef]
66. Ullah, S.; You, Q.; Ullah, W.; Hagan, D.F.T.; Ali, A.; Ali, G.; Zhang, Y.; Jan, M.A.; Bhatti, A.S.; Xie, W. Daytime and nighttime heat wave characteristics based on multiple indices over the China–Pakistan economic corridor. *Clim. Dyn.* **2019**, *53*, 6329–6349. [CrossRef]
67. Monteiro, J.M.; Caballero, R. Characterization of extreme wet-bulb temperature events in southern Pakistan. *Geophys. Res. Lett.* **2019**, *46*, 10659–10668. [CrossRef]
68. Saleem, F.; Zeng, X.; Hina, S.; Omer, A. Regional changes in extreme temperature records over Pakistan and their relation to Pacific variability. *Atmos. Res.* **2021**, *250*, 105407. [CrossRef]
69. Malik, S.M.; Awan, H.; Khan, N. Mapping vulnerability to climate change and its repercussions on human health in Pakistan. *Global. Health* **2012**, *8*, 31. [CrossRef]
70. Im, E.; Pal, J.S.; Eltahir, E.A.B. Deadly heat waves projected in the densely populated agricultural regions of South Asia. *Sci. Adv.* **2017**, *3*, e1603322. [CrossRef]
71. Saeed, F.; Almazroui, M.; Islam, N.; Khan, M.S. Intensification of future heat waves in Pakistan: A study using CORDEX regional climate models ensemble. *Nat. Hazards* **2017**, *87*, 1635–1647. [CrossRef]
72. Aslam, A.Q.; Ahmad, S.R.; Ahmad, I.; Hussain, Y.; Hussain, M.S. Vulnerability and impact assessment of extreme climatic event: A case study of southern Punjab, Pakistan. *Sci. Total Environ.* **2017**, *580*, 468–481. [CrossRef]
73. Khan, N.; Shahid, S.; Ismail, T.; Ahmed, K.; Nawaz, N. Trends in heat wave related indices in Pakistan. *Stoch. Environ. Res. Risk Assess.* **2019**, *33*, 287–302. [CrossRef]
74. Saddique, N.; Khaliq, A.; Bernhofer, C. Trends in temperature and precipitation extremes in historical (1961–1990) and projected (2061–2090) periods in a data scarce mountain basin, northern Pakistan. *Stoch. Environ. Res. Risk Assess.* **2020**, *34*, 1441–1455. [CrossRef]
75. Nasim, W.; Amin, A.; Fahad, S.; Awais, M.; Khan, N.; Mubeen, M.; Wahid, A.; Rehman, M.H.; Ihsan, M.Z.; Ahmad, S.; et al. Future risk assessment by estimating historical heat wave trends with projected heat accumulation using SimCLIM climate model in Pakistan. *Atmos. Res.* **2018**, *205*, 118–133. [CrossRef]
76. Herring, S.C.; Hoell, A.; Hoerling, M.P.; Kossin, J.P.; Iii, C.J.S.; Stott, P.A. Explaining extreme events of 2015 from a climate perspective. *Bull. Amer. Meteorol. Soc.* **2016**, *97*, S1–S145. [CrossRef]
77. Masood, I.; Majid, Z.; Sohail, S.; Zia, A.; Raza, S. The deadly heat wave of Pakistan, June 2015. *Int. J. Occup. Environ. Med.* **2015**, *6*, 247–248. [CrossRef]